Opt Quant Electron (2009) 41:787–793
DOI 10.1007/s11082-010-9392-0

Transient and steady state lateral charge transport in polymeric semiconductors

Abhay K. Tiwari · N. S. Vidhyadhiraja

Received: 14 October 2009 / Accepted: 8 May 2010 / Published online: 25 May 2010

Abstract The Lateral photovoltaic effect (LPE) has been used as an effective tool to probe the dynamics of photogenerated charge carriers in conjugated polymer based optoelectronic devices. In this paper, we analyze the time-dependence of LPE in a position sensing device geometry using a discrete circuit equivalent model coupled with a spreading impedance approach. We elucidate the dependence of the lateral photovoltage (LPV) on the position, intensity and the modulation frequency (ω_c) of the light beam. Previous experimental results for the position and ω_c dependence of the LPV in the steady state are successfully reproduced within the present approach. We predict a clear knee-like feature in the transient regime of the LPV for high photocurrent values. This feature prompts us to propose that the response time of the organic position sensing device decreases sharply with increasing incident intensity.

Keywords Lateral photo voltage · Transient response · Spreading impedance

1 Introduction

Conjugated polymer based organic semiconductors have been explored extensively in optoelectronic applications as they offer tremendous advantages in processing and fabricating procedures. The lateral photovoltaic effect (LPE) has been used to probe the photogenerated charge carrier dynamics in optoelectronic devices (Malliaras and Friend 2005; Forrest 2004; Burroughes et al. 1990). In earlier work from our group (Kabra et al. 2007, 2008), a spreading impedance approach to a discrete circuit equivalent model (Fynn et al. 1995) was found to

A. K. Tiwari (✉)
Chemistry and Physics of Materials Unit, Jawaharlal Nehru Centre for Advanced Scientific Research, Bangalore 560064, India
e-mail: abhayk@jncasr.ac.in

N. S. Vidhyadhiraja
Theoretical science Unit, Jawaharlal Nehru Centre for Advanced Scientific Research, Bangalore 560064, India
e-mail: raja@jncasr.ac.in

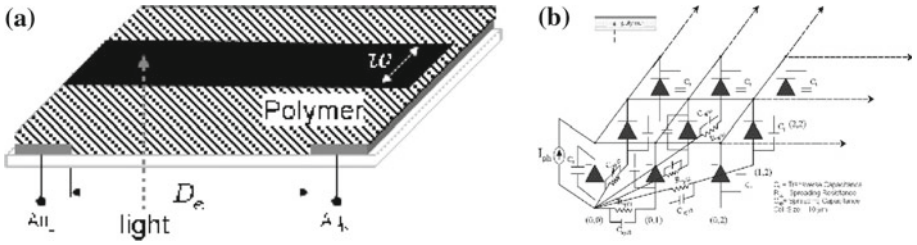

Fig. 1 **a** A typical position sensing device, **b** equivalent circuit spreading impedance network model of the polymeric Schottky device

provide an excellent description of the experimental results in the steady state of a polymeric position sensing device. However, the analysis carried out in that work had certain limitations. The equations were linearized and solved in the frequency domain. Further, the Fourier frequency was equated to the modulation frequency of the incident light beam. So the limitations resulting from such an analysis are three-fold: The first and foremost being that transient dynamics information could not be obtained. Such studies are very important in understanding experiments such as time-of-flight measurements (Campbell et al. 2001; Valasaki et al. 2002; Choulis et al. 2004). Secondly, linearization of the equations imply that non-linear effects that could arise at higher incident intensities etc cannot be observed; and finally comparison to experiments could be carried out only for the spatial dependence of the LPV and for relatively low light intensities.

In this work, we have taken a different route for analysing our model that lets us overcome all the three limitations mentioned above. We study the model directly in the time domain without linearizing the equations. This helps us to get the spatiotemporal dependence of the lateral transport within a single framework. Further, in previous work, the recombination effects across the Schottky diode back contact were treated in the linear regime. Such an approximation is naturally incorrect at high incident light intensities. In this work, this limitation has also been overcome, thus yielding specific predictions for the non-linear response of the device.

The paper is structured as follows: In the following section, we describe the model and formalism. Next in Sect. 3, we describe the numerical procedure followed by us for the solution of model equations. In Sect. 4, we present our results and discussions. We conclude in the final section.

2 Model and formalism

The model (Kabra et al. 2007, 2008) aims to describe the lateral photovoltaic effect in a polymeric semiconductor based position sensing device as shown in Fig. 1a. The device structure consists of a polymer-Al Schottky junction with front pair of Au electrodes. The polymers used were poly(3-hexylthiophene) (P3HT) and poly-[2-methoxy,5-(2-ethylhexoxy)-1,4-phenylene vinylene](MEHPPV). The lateral photovoltage is measured across the Au electrodes. The lateral potential profile $\phi_{ph}(r)$ has been discretized on a square lattice of nodes where potential at each node is denoted by ϕ_m (Fig. 1b). The current through each node m has a transverse and lateral component. The transverse component comprises reinjection of minority charge carriers made possible by the barrier reduction in the Schottky junction. This has been modeled as a combination of diode and capacitive current which are given as following.

$$I_{D,m}^{T} = I_s \left[\exp\left(\frac{q\phi_m}{k_B T}\right) - 1 \right] \tag{1}$$

$$I_{C,m}^{T} = C_t \frac{d\phi_m}{dt} \tag{2}$$

For the illuminated nodes, the photogenerated majority charge carriers add to the transverse incoming current and are represented by a current source $I_{ph,m}$. The lateral current has two components: a resistive component I_R^L arising due to the disorder scattering of the charge carriers, and a capacitive component I_C^L which is attributed to the presence of traps that affect the mobility of the charge carriers. The resistive and capacitive component of the current from node m to n are given as:

$$I_R^L = \frac{\phi_m - \phi_n}{R_{sp}(m,n)} \tag{3}$$

$$I_C^L = C_{sp}(m,n) \frac{d(\phi_m - \phi_n)}{dt} \tag{4}$$

where R_{sp} and C_{sp} are the internode spreading resistance and capacitance respectively. In disordered polymers, the number of scattering centers increase far more rapidly with internode distance $r_{mn} = |r_m - r_n|$ than their inorganic crystalline counterparts. The effect of such a disordered morphology can be very effectively modeled by a spreading function

$$g(r_{mn}) = \exp\left[\left(\frac{r_{mn}}{\zeta} \right)^{\alpha} \right] \tag{5}$$

where α is the stretching exponent of the spreading function and ζ is the length scale which is charcteristic of the material under consideration. Using the above mentioned spreading function the internode resistance and capacitance are given as follows:

$$R_{sp} = R_s g(r_{mn}) \tag{6}$$

$$C_{sp} = \frac{C_s}{g(r_{mn})} \tag{7}$$

where R_s and C_s are the sheet resistance and sheet capacitance respectively. Now we have divided the set of nodes into four mutually exclusively sets depending on whether the node is illuminated or not, and whether it is a part of electrode or not. (i) S_{IL}: set of nodes that are illuminated, (ii) S_{NIL}: set of non-illuminated non-electrode nodes (iii) S_{LE}: set of nodes coincident with left electrodes, and (iv) S_{RE}: set of nodes coincident with right electrodes. A straightforward application of the Kirchhoff's current law yields the potentials for all the nodes. The equations are as follows:

For dark or non-illuminated nodes, $m \in S_{NIL}$

$$I_s \left[\exp\left(\frac{q\phi_m}{k_B T}\right) - 1 \right] + C_t \frac{d\phi_m}{dt} + \sum_{l \in S_{IL}} \left[\frac{\phi_m - \phi_l}{R_{sp}(l,m)} + C_{sp}(l,m) \frac{d(\phi_m - \phi_l)}{dt} \right] = 0 \tag{8}$$

For illuminated nodes, $l \in S_{IL}$,

$$I_s \left[\exp\left(\frac{q\phi_l}{k_B T}\right) - 1 \right] + C_t \frac{d\phi_l}{dt} + I_{ph,l} + \sum_{\substack{m \in S_N \\ m \neq l}} \left[\frac{\phi_l - \phi_m}{R_{sp}(l,m)} + C_{sp}(l,m) \frac{d(\phi_l - \phi_m)}{dt} \right] = 0 \tag{9}$$

All the nodes on the electrodes would be equipotential, thus for the left electrode potential Φ_L,

$$N_L I_s \left[\exp\left(\frac{q\Phi_L}{k_B T}\right) - 1\right] + N_L C_t \frac{d\Phi_L}{dt} + \sum_{\substack{m\in S_{LE} \\ l\in S_{IL}}} \left[\frac{\Phi_L - \phi_l}{R_{sp}(m,l)} + C_{sp}(m,l)\frac{d(\Phi_L - \phi_l)}{dt}\right] = 0 \tag{10}$$

Similarly, for the right electrode potential Φ_R,

$$N_R I_s \left[\exp\left(\frac{q\Phi_R}{k_B T}\right) - 1\right] + N_L C_t \frac{d\Phi_R}{dt} + \sum_{\substack{m\in S_{RE} \\ l\in S_{IL}}} \left[\frac{\Phi_R - \phi_l}{R_{sp}(m,l)} + C_{sp}(m,l)\frac{d(\Phi_R - \phi_l)}{dt}\right] = 0 \tag{11}$$

where N_L and N_R are the number of left and right electrode nodes respectively. By solving (8)–(11) we can determine LPV (ΔV_{ph}) defined by

$$\Delta V_{ph}(l,t) = |\Phi_L - \Phi_R| \tag{12}$$

The advantages of the method adopted here over the previous work (Kabra et al. 2007, 2008) is that we can not only capture the transient profile of the response but also the non-linearity by keeping the exponential form of the diode current, i.e by not linearizing the exponential.

In an earlier study (Kabra et al. 2008), we linearized the exponentials in Eqs. (8)–(11), and converted them to coupled linear equations using Fourier transform. Additionally, we chose to solve the equations for a single frequency, namely the modulation frequency ω_c. In this work, we do not make such approximations. The Eqs. (8)–(11) are directly evolved in time using a simple first order finite difference technique. The resulting equations may be cast into a matrix format which is then treated using sparse matrix routines. Although we have considered several functional forms for the incident photocurrent, such as the square wave form, saw tooth form etc, in this work we report results for the square wave form only. In each case the dependence of the lateral photovoltage on the amplitude and the modulation frequency was investigated.

3 Results and discussion

Since the method adopted in this work has been implemented for the first time, we would like to benchmark it with our previous method and verify that we do indeed reproduce the results obtained previously. In order to carry out the benchmarking we employ a dc incident photocurrent and plot the steady state lateral photovoltage as a function of the beam position in Fig. 1 for two devices of different form factors L/W. The other parameters such as the sheet resistance, junction capacitance, I_s and the spreading function parameters are the same as those in our earlier work (Kabra et al. 2007, 2008). A direct superposition of theory onto the experimental results from Kabra et al. (2007) and a comparison to Fig. 2a and b in Kabra et al. (2008) shows that the present method does yield consistent results for the spatial profile of the LPV.

In what follows, we will consider a device with dimensions $0.7 \times 0.5\,\mathrm{mm}^2$ implying a form factor $L/W = 1.4$, and focus on the transient response of the device to a dc as well as an ac incident photocurrent. To see if the functional form of the LPV and the time scales involved are dependent on the amplitude of the (dc) photocurrent, we compute the LPV response to

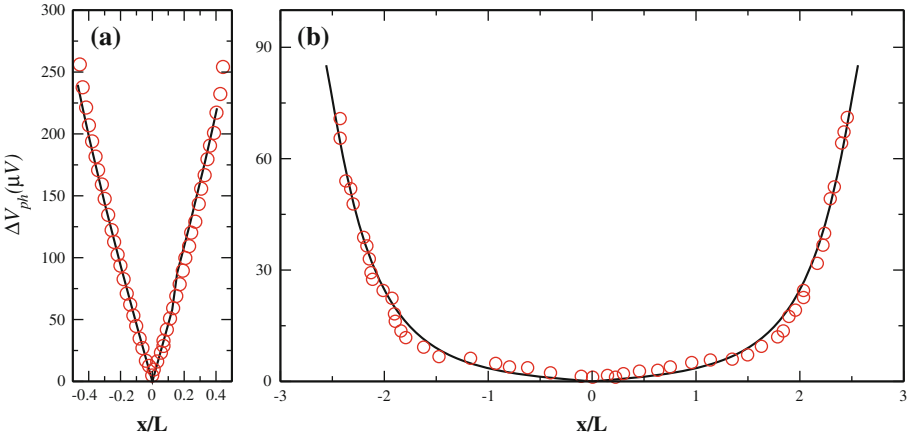

Fig. 2 Steady state LPV *vs.* beam position. **a** $L/W \sim 1$, **b** $L/W \gg 1$. The *solid line* is the theory and *circles* are the experimental values for similar form factor devices

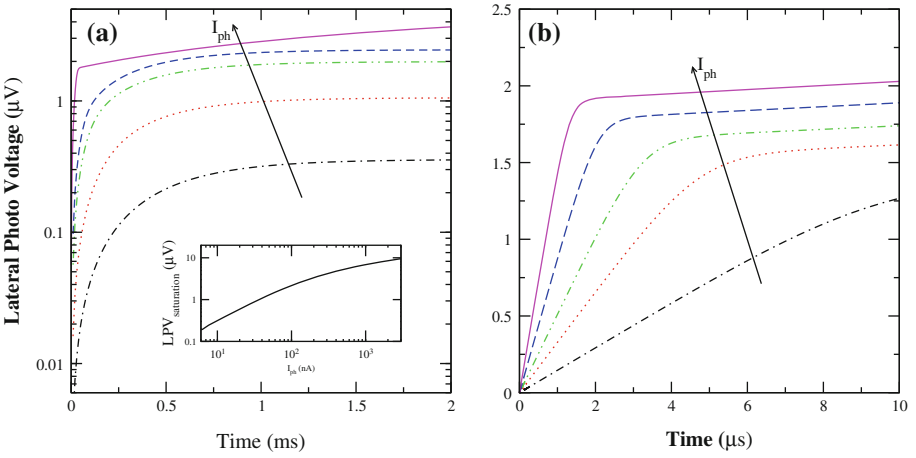

Fig. 3 **a** Transient values of the LPV as a function of different values of the incident photocurrent. The inset shows the LPV-saturation value as a function of the incident photocurrent. We can see a clear change in the slope. **b** knee voltage in the transient LPV is highlighted

a series of increasing I_{ph} values. The result is shown in Fig. 3. We see that the time scales do depend significantly on the amplitude of the photocurrent. The saturation value of the LPV as a function of the incident photocurrent (inset, Fig. 3) shows a clear departure from linear reponse for larger I_{ph}. Such non-linearity is seen to manifest itself in the time-dependence of the LPV as well. A careful observation of the LPV(t) in Fig. 3 for higher I_{ph} shows a knee-like feature, that is completely absent at low intensities. In panel (b) of Fig. 3, we zoom on the knee feature, and show the LPV(t) for a few relatively high I_{ph} values. It is seen that this knee feature occurs earlier for higher I_{ph}. It is clear that this feature indicates that the response time of the device decreases with increasing incident intensity. Note that the t_{knee} is of the order of microseconds, while the saturation occurs on a millisecond time scale (for the present set of parameters). This suggests that the initial rapid rise at high photocurrents could be utilized to obtain fast response in a polymeric Schottky diode device.

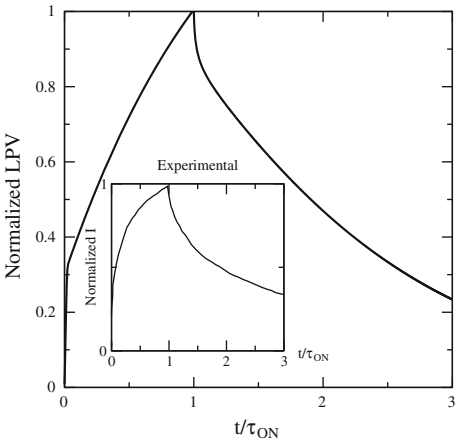

Fig. 4 Transient on/off profile of the normalized LPV. In the inset is shown the experimentally measured photocurrent (data from Kabra et al. 2004; see text for description)

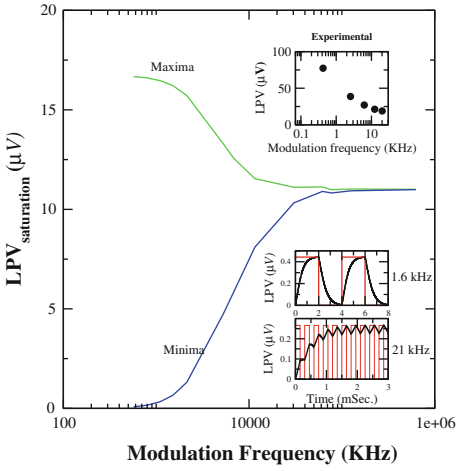

Fig. 5 Maximum and minimum value of steady state response at various frequencies. In the upper set the experimental curve is shown (Kabra et al. 2008) and in the lower ones the evolution of LPV(t) at a higher and a lower frequency

In Fig. 4, we show the time dependent and normalized (with respect to its maximum value) LPV as a function of time for a dc incident light which is turned ON at $t=0$ and switched off at $\tau_{\rm ON} = 200\,$s. The inset shows an experimentally measured $I_{ph}(t)$ (Kabra et al. 2004) between the two gold electrodes with one of the electrodes shorted with the *Al* electrode. The experiment employs an external load resistance to measure the output current, implying that the current is just proportional the LPV. We observe several unusual features in the experiment that are reproduced within the theory. Firstly, there is an obvious asymmetry between the rise and decay of the experimental LPV. A rapid initial rise followed by a gradual rise (giving rise to the knee-like feature) is seen in experiment as well as theory. The decay is far more gradual than the rise, reflecting the interplay of various processes involving multiple time scales. We find that this asymmetry between the rise and decay occurs for high photocurrents ($\gtrsim$10 nA), and for $\tau_{\rm ON}$ that is comparable to the $t_{\rm knee}$. As explained below (see Fig. 3) high photocurrents give rise to the knee-feature that reflects a very rapid rise. Switching off the incident light soon after $t_{\rm knee}$ gives rise to the slow decay.

Finally, we show the dependence of the steady state response (SSR) on the modulation frequency of the incident photocurrent. In Fig. 5 we show the maximum and the minimum of

the SSR as a function of the modulation frequency. It is seen that the maximum of the SSR decreases sharply with increasing ω_c. This is seen in experiments as well (Kabra et al. JAP) and thus provides further support to the theory presented here. In addition, the result shows that the maximum and the minimum converge to a common value at high frequencies. The insets show the actual LPV(t) for a low ω_c and a high one.

4 Conclusion

In this work, we present a consistent framework for exploring the transient and non-linear characteristics of lateral transport in organic polymeric devices. The theory presented here is benchmarked against earlier theoretical and experimental results. The agreement is seen to be quite good. We make a few predictions as well that can be tested by further experiments. One of them is the knee-like feature that is purely a non-linear response of the device to high photocurrents. The second is the deviation from linearity of the steady state LPV as a function of photocurrent. Further experimental investigations to test these predictions are presently going on in our group. We are also extending the theory further to make quantitative comparisons to experiment as well as investigate the effect of other parameters such as beam profile, morphology, junction capacitance and trap densities. We hope that our study will be helpful for the simulation and prediction of new designs of organic optoelectronic devices.

Acknowledgments The authors would like to thank Prof. C.N.R. Rao for generous travel funding through ICMS, which made it possible for one of us (AKT) to present this work at NUSOD-2009. We would also like to thank Prof. K.S. Narayan for insightful comments and very fruitful discussions.

References

Burroughes, J. et al.: The first polymer LEDs. Light-emitting-diodes based on conjugated polymers. Nature **347**, 539–541 (1990)

Campbell, J., Bradley, D.D.C., Antoniadis, H.: Dispersive electron transport in an electroluminescent polyfluorene. Appl. Phys. Lett. **79**, 2133–2135 (2001)

Choulis, A. et al.: High ambipolar and balanced carrier mobility in regioregular poly(3-hexylthiophene). Appl. Phys. Lett. **85**, 3890–3892 (2004)

Forrest, S.R.: The path to ubiquitous and low-cost organic electronic appliances on plastic. Nature **428**, 911–918 (2004)

Fynn, A., Bajaj, J., Farone, L.: A discrete element model of laser . . . HgCdTe photodiodes. IEEE Trans. Elect. Dev. **42**, 1775–1782 (1995)

Kabra, D., Singh, T.B., Narayan, K.S.: Semiconducting-polymer-based position-sensitive detectors. Appl. Phys. Lett. **85**(21), 5073–5075 (2004)

Kabra, D., Shriram, S., Vidhyadhiraja, N.S., Narayan, K.S.: Charge carrier dynamics in organic semiconductors by position dependent optical probing. J. Appl. Phys. **101**, 064510 (2007)

Kabra, D., Verma, J., Vidhyadhiraja, N.S., Narayan, K.S.: Model for studies of lateral photovoltaic effect in polymeric semiconductors. IEEE Sensors. Journal. **8**, 1663–1671 (2008)

Malliaras, G., Friend, R.H.: An organic electronics primer. Phys. Today **58**, 53–58 (2005)

Valasaki, L., Moreira, M., Micaroni, L., Hummelgen, I.A.: Charge injection and transport in electrochemical films of poly(3-hexylthiophene). J. Appl. Phys. **92**, 2035 (2002)